

Pricing and Restoring Natural Capital: A Case-Study on Mining and Vegetation

E4S White Paper - **TECHNICAL APPENDIX**

Edoardo Chiarotti¹, Jean-Philippe Bonardi², Jean-Pierre Danthine³, Dario Scalabrin⁴, and Filippo Trapanese⁵

July 2023

© Enterprise for Society (E4S) Center, 2023

We are grateful to Marti Bosch (EFPL), Dries Cornilly (Asteria Obviam), Quentin Gallea (E4S, UNIL), Pernille Holtedahl (Imperial College Business School), Florence Hugard (E4S, UNIL), Sascha Nick (EFPL), Boris Thurm (E4S, EPFL), Michele Volpi (ETH), and participants at seminars and conferences, for their valuable comments and feedback.

Enterprise for Society (E4S) is a joint venture of the University of Lausanne through its Faculty of Business and Economics (UNIL-HEC), the Institute for Management Development (IMD) and the Ecole Polytechnique Fédérale de Lausanne (EPFL), under the stewardship of its College of Management of Technology, with the mission of spearheading the transition towards a more resilient, sustainable and inclusive economy. E4S is committed to training the next generation of leaders, inspiring economic and social transformation, and promoting change by strengthening start-ups and boosting innovation.

¹ Enterprise for Society Center, University of Lausanne (HEC)

² Enterprise for Society Center, University of Lausanne (HEC)

³ Enterprise for Society Center, EPFL

⁴ Enterprise for Society Center, Zurich Insurance

⁵ Enterprise for Society Center, Quantis

TABLE OF CONTENTS

Table of contents	2
1 Measuring Vegetation Loss with Satellite Images	3
1.1 Satellite Images	3
1.2 Vegetation Indexes	5
2 Checks for Antamina	6
3 Supplementary Images for the Instituto Terra.....	8
4 Images and Figures for Fountain Wildfire	9
5 Instituto Terra: Financial Reports.....	12
6 References	13

1 MEASURING VEGETATION LOSS WITH SATELLITE IMAGES

This study uses satellite imagery to analyse the impact of companies on vegetation. As a starting point, we retrieve the satellite images around the location of these companies' physical assets. We then use these images to compute the Enhanced Vegetation Index (EVI), which is an image-based measure for vegetation density. By comparing the EVI scores at two different periods, and also across different locations, we provide a first-step methodology to assess the impact of businesses on nature, either negative or positive.

Satellite images - also that date back to the 1980s - have become widely available. The advancement of remote sensing and Geographic Information System (GIS) technology allows to monitor the changes in land use and cover at the global, continental, and national level, for both their spatial, temporal, and spectral characteristics [1]. In the last decades, researchers started using satellite images to track the evolution of forests, and more broadly vegetation. For example, [2] use satellite images to show that, between 2000 and 2012, Earth lost around 2.3 million km² of forests, and gained barely 0.8 million km².⁶ In this paper we build upon the techniques used in this literature and use satellite images to compute an index for vegetation density and link it to companies' activities.

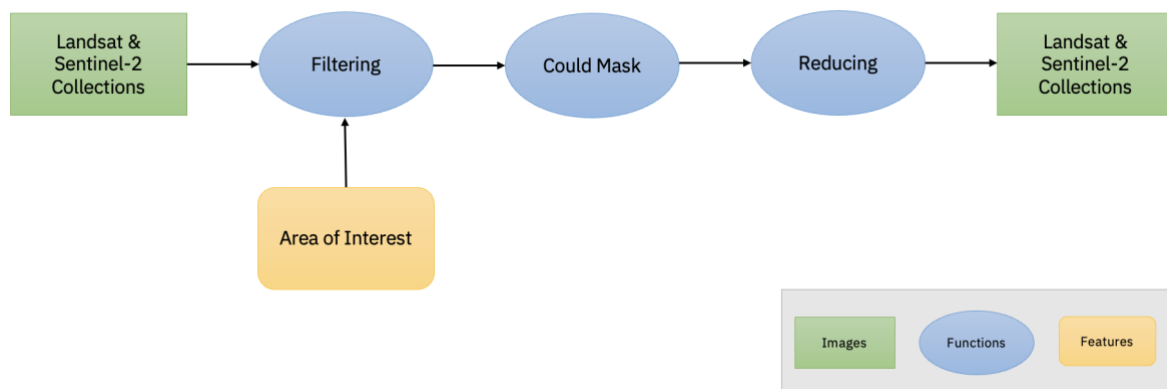
1.1 SATELLITE IMAGES

The database for satellite images we rely on is called Landsat 5, which has daily images at 30-meter resolution over 1984-2012. We retrieve historical satellite images of selected locations using Google Earth Engine (GEE). GEE is a free service for non-commercial use and it is easy to integrate into Python or JavaScript code [3]. GEE provides a large catalogue of satellite images and geospatial datasets with planetary-scale analysis capabilities. In particular, we use pictures from a satellite-image database called Landsat 5, which provides extensive and accurate data on Earth's land surface for nearly three decades (March 1984 – May 2012), the longest-operating Earth observation satellite [4]. Landsat allows us to study locations around business activities far back in time, which is key considering that companies made large use of natural resources already in the 1980s [5]. While Landsat has the advantage of providing this historical perspective, it has the drawback that the resolution is at "only" 30 meters, which is not as high as the newest databases such as Sentinel 2 [7]. However, a 30-meter resolution is sufficient to build the vegetation index we use in this study.

Image processing includes filtering, cloud mask and reducing. Our goal is to have a representative image of a location before and after the physical asset, e.g. a mine, was built. Given the different atmospheric conditions and seasonality, we need to apply a disaggregating 3-step process, represented in Figure 1. The final output is a composite, single image that is created by combining multiple images within a time window of the same area.

⁶ This and other databases allowed the creation of open-source web applications to monitor global forests in real-time, such as [Global Forest Watch \(GFW\)](#).

Figure 1: Filtering and Reducing Satellite Images



Notes. This figure reports a representation of the process of (i) filtering satellite images, (ii) reducing them by applying a cloud-mask algorithm from Google Earth Engine called *SimpleLandsatCloudScore*. The input is a set of images from a time window and the output is a single, reduced image, representative of the time window considered.

1.1.1 Filtering

We define a circular area with a radius of 3 kilometres around the physical asset of interest. The starting point is defining a circular area of interest around the coordinates of the company's physical asset, such as a mining site for an extraction company. As radius for this circle area we chose 3 kilometres, which is sufficient to observe the status of vegetation around a large mining site.⁷

We use image reduction to obtain 2 images, one before and one after the physical asset was built. We then collect the images available in Landsat 5 for each time window - so called image collection. The extent of the time window depends on the exercise we run. In most of the analysis, we aim to observe what happens before and after a determined physical asset is built. We thus retrieve all images in, respectively, the 3 years before the asset was built and the last three years of the period covered by Landsat 2 (2009-2012).

1.1.2 Cloud Mask and Reducing

The reduction process uses a cloud mask to minimize the presence of clouds. Clouds can obscure the satellite view of the ground and make it difficult to see what is happening in some areas. To address this issue, we use a processing method called cloud mask, which identifies and separates clouds in satellite images. Specifically, we consider the set of images of the same area we have in our filtered collections. We then apply the *SimpleLandsatCloudScore* algorithm - a pre-built algorithm provided by GEE - which assigns a cloud score to each pixel of each image in the collection.⁸ The algorithm then proceeds with a reducing process by selecting the lowest possible range of cloud scores at each point and takes the pixel with the median values across these scores.

⁷ There is no standard to pick the area's radius, and 3 kilometers is just an example. Since each image has a 30m resolution, we could not take any area smaller than 30 meters, otherwise no details would be detectable. In future work, we will automatize the selection of this parameter considering the perimeter of mining sites.

⁸ For more details on the algorithm, see here: <https://developers.google.com/earth-engine/apidocs/ee-algorithms-landsat-simplecomposite>.

The final composite image is composed of several bands, which are separate channels of image data. For the scope of our analysis, we are interested in the Red (R), Green (G), Blue (B), and near-infrared (NIR) bands. The first three represent the intensity of one of the primary colours of light, i.e., red, green, or blue, while the infrared channel captures wavelengths that are longer than those of visible light and are not visible to the human eye. Combining these channels in different proportions makes it possible to produce a wide range of colours. For instance, an RGB image is a close representation of what a human eye would see.

1.2 VEGETATION INDEXES

The most widely used vegetation index is the Normalized Difference Vegetation Index (NDVI). We use the bands in the composite images to build an index that measures the density of vegetation. The most widely used index in the literature is the Normalized Difference Vegetation Index (NDVI) (e.g. [7]). The NDVI was developed in the 1970s and uses the amounts of light in the infra-red and red bands reflected by the vegetation and captured by the satellite. Specifically, the NDVI is calculated at the pixel level from the infra-red and red reflectance values as follows:

$$NDVI = \frac{NIR - R}{NIR + R} \quad (1)$$

The leaf's mesophyll scatters near-infrared light, while the chlorophyll absorbs red light. The NDVI uses the reflectance values to grasp the process of photosynthesis. The mesophyll leaf structure scatters near-infrared light, while the chlorophyll absorbs red light [8]. So the higher the difference between NIR and R light, the higher is the photosynthesis in the considered pixel, and denser is the vegetation. The NDVI values for a particular pixel range from -1 to +1, with negative values indicating the absence of green foliage and values close to +1 indicating denser and healthier vegetation [9].

As the NDVI is sensitive to changes in natural habitats unrelated to vegetation, we consider the corrected Enhanced Vegetation Index (EVI). While the NDVI is widely used because of its simplicity, and ability to recognize vegetated areas from other surface types [10], it presents some issues, such as reflectance problems with thick clouds and wet soils.⁹ The literature has proposed alternative indexes that take care of some of these issues, such as the Soil-Adjusted Vegetation Index (SAVI) [14], the Atmospherically Resistant Vegetation Index (ARVI) [15], and the Enhanced Vegetation Index (EVI) [14].¹⁰ For our analysis we rely on the EVI, which is a vegetation index developed by NASA in the early 2000s as an improvement over the NDVI. Since the launch of the Moderate-resolution Imaging Spectroradiometer (MODIS), NASA adopted the EVI as the new standard to assess vegetation. Like the NDVI, the EVI is calculated at the pixel level using the difference between the near-infrared and red wavelengths of light

⁹ First, the NDVI is affected by the amount of light scattered in the atmosphere, which is more significant in the R region than in the NIR region. This means that NDVI values calculated using data recorded at the top of the atmosphere are generally lower than those calculated using surface reflectance [11]. Second, while thick clouds can be easily excluded, thin or small clouds smaller than the area considered by the satellite sensors can significantly impact the NDVI measurements. Additionally, cloud shadows can affect NDVI values and lead to misinterpretations [12]. Finally, when the soil becomes wet, it tends to darken in color. This happens because when the moisture levels of the soil in an area change due to rain or evaporation, the soil absorbs more light in different parts of the spectrum. As a result, the NDVI can change, while the vegetation density remains the same [13].

¹⁰ These limitations can be addressed by forming composite images from temporal data. The technique minimizes the impact of clouds, reduces the effects of reflected light and oblique viewing angles, and minimizes the effects of aerosols and water vapor on the measurements [16].

reflected by plants, but it includes additional adjustments to account for atmospheric effects and the influence of soil background. Precisely, the EVI is computed in the following way [4]:

$$EVI = G \times \frac{NIR - R}{NIR + C_1R - C_2B + L} \quad (2)$$

NIR, R, and B are the full (or partially), atmospheric corrected surface reflectance for, respectively, near-infrared, red and blue. L is the canopy background adjustment for correcting the nonlinear, differential NIR and R radiant transfer through a canopy. C1 and C2 are the coefficients of the aerosol resistance term (which uses the blue band to correct for aerosol influences in the red band). G is a gain or scaling factor. The coefficients adopted for the MODIS EVI algorithm are L = 1, C1 = 6, C2 = 7.5 and G = 2.5 [17].

The EVI ranges from -1 to 1, with positive values indicating the presence of vegetation - healthy tropical forests have values around 0.7. Like the NDVI, the EVI ranges from -1 to 1. The literature reports that peak EVI values for deserts (no vegetation), savanna biomes (some vegetation) and tropical forests (lots of vegetation) are, respectively, 0.1, 0.4 and 0.7 [14], and that healthy vegetation is usually between 0.5 and 0.8 EVI points [18]. However, as EVI values can vary largely between different natural habitats and vegetation types, the thresholds for what we can call “healthy vegetation” might vary significantly across locations.

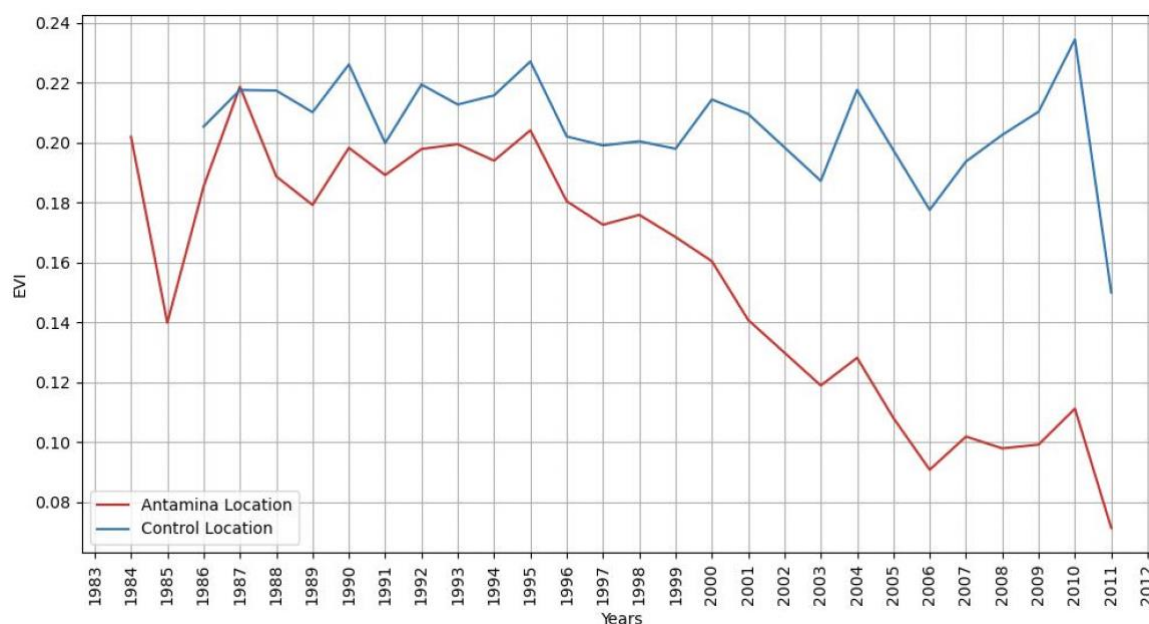
In our analysis, we compute the EVI for each pixel of the selected composite images. We finally obtain an image-level EVI by averaging the EVI values for all pixels in the image.

2 CHECKS FOR ANTAMINA

This section reports the robustness checks for the EVI values for the Antamina site, reported in the white paper in Table 1. Here, table 1 reports the results, both for the baseline (first columns) and the performed checks (other columns).

Figure 2 shows the evolution of the EVI index over time between the Antamina location and the control location. For this control location to be a “good” control, there must be no major differences in the trends of the EVI before and after the mine was built. To visualize this, we compute the yearly EVI by reducing satellite images for each year, and we plot the time series in Figure 2.

Figure 2: Enhanced Vegetation Index - Trends in the Antamina and Control Locations



Notes. This figure reports yearly values for the EVI index for both the Antamina location (blue), and a control location (red) of similar altitude that is 7.1 kilometres away from the Antamina location. The yearly values are obtained by compressing all images from the same season available in each considered year. As we do not have many satellite images for 2002, the value for 2002 is interpolated with an average of values in 2001 and 2003.

The red line is the yearly time series of the EVI in the Antamina location, while the blue line is the yearly time series of the EVI in the control location.¹¹ From the red line we can see that the vegetation in the Antamina location started declining in 1998, which is when the consortium of companies started the drilling operations. On the other hand, the blue line shows that vegetation in the control location remained approximately constant throughout the considered period.¹² This anecdotal evidence suggests that the control we are using could be considered a good control, as the only difference in the trends appear to be around the construction of the mine.

Table 1 reports the robustness checks for the Antamina and control locations. The table shows that result can change when we vary the parameters of our methodology. First, a reduction in the considered area's radius from 3 to 2 kilometres produces a larger adjusted change in the EVI value (-0.1046 in column 2). This is intuitive as, likely, the captured area focuses more on the location of the extraction site per se and thus excludes surrounding vegetation that survived. Second, an increase in the considered area's radius from 3 to 4 kilometres produces a smaller adjusted change in the EVI value (-0.0725 in column 3). The same logic holds here, as the larger the area around the mine, the more untouched vegetation is included, and therefore the milder is the reduction in the EVI. In future work, we will work to

¹¹ In the figure we do not report the year 2002, which has very few satellite images available for these locations. The resulting EVI is imprecise and not indicative.

¹² The yearly bumps are mainly due to the availability of images by year. When the availability is low, the resulting EVI can be imprecise. While Figure 4 is useful for representation purposes, in our baseline comparison we do not consider yearly values, but we focus on before and after values, computed as explained before.

include the area interested in the mining activities by relying on official land-ownership data, or image-recognition techniques.

Table 1: Robustness Checks for Adjusted Differences in EVI for Antamina

	Rad: 3000 Bef: 94-97 Aft: 09-12	Rad: 2000 Bef: 94-97 Aft: 09-12	Rad: 4000 Bef: 94-97 Aft: 09-12	Rad: 3000 Bef: 84-87 Aft: 09-12	Rad: 3000 Bef: 95-97 Aft: 10-12	Rad: 3000 Bef: 93-97 Aft: 08-12
Antamina						
Before	0.1916	0.1617	0.2005	0.2163	0.1857	0.196
After	0.0995	0.0513	0.1258	0.0995	0.0757	0.0965
Diff	-0.0921	-0.1104	-0.0747	-0.1168	-0.11	-0.0995
Diff %	-48.0689	-68.2746	-37.2569	-53.9991	-59.2353	-50.7653
Control						
Before	0.2144	0.2101	0.2102	0.2266	0.2093	0.2176
After	0.2122	0.2043	0.208	0.2122	0.1579	0.2051
Diff	-0.0022	-0.0058	-0.0022	-0.0144	-0.0514	-0.0125
Diff %	-1.0261	-2.7606	-1.0466	-6.3548	-24.5581	-5.7445
Diff-in-Diff	-0.0899	-0.1046	-0.0725	-0.1024	-0.0586	-0.087

Notes. Column 1 reports the baseline figures. Columns 2 and 3 report the figures obtained by changing the radius of the area of interest from 3 km to, respectively, 2 km and 4 km. Column 4 shows the results when we change the time window used to compute the EVI value for before the mine was built from a time window just before the mine was built (1994-97) to a time window at the beginning of our dataset (1984-87). Columns 5 and 6 report the results as we change the time windows to obtain the EVI values from 3-year spans (1994-97 and 2009-12) to, respectively, 2-year spans (1995-1997 and 2010-2012) and 4-year spans (1993-97 and 2008-12).

Third, column 4 shows what happens when we change the time window to obtain the image representative of the area before the mine was built. If we move this window from just before the mine was built (1994-97, baseline) to the first available period in the dataset (1984-87), the negative adjusted EVI change is larger (-0.1024). This is also intuitive, as moving the window at the beginning of the dataset implies including in the estimate any natural vegetation loss happened before the mine was built. This motivates further our choice of using a time window that just precedes the construction of the mine in our baseline. In future work, we will work to obtain the construction date of mining sites, so we can address this degree of error for company-level results.

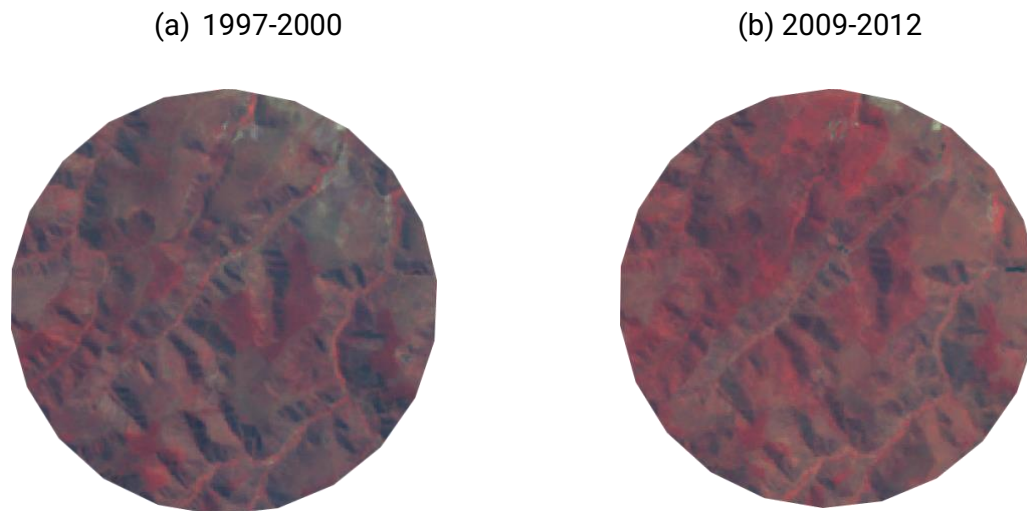
Finally, in columns 5 and 6 we show what happens when we change the length of the time windows used to compute the respective composite satellite images. Specifically, columns 5 and 6 report the figures and adjusted EVI change for 2-year windows (1995-97 and 2010-12) and 4-year windows (1993-97 and 2008-12). Results change mainly because of changes in the control location for the 2-year window, which can be quite sensitive as there can be few available satellite images in that more limited time frame. On the other hand, 4-year windows' results are more aligned with the baseline.

3 SUPPLEMENTARY IMAGES FOR THE INSTITUTO TERRA

Here we report added images for the Instituto Terra. Figure 3 reports the infrared composite images for the circular area of radius of 3 km that we consider around the reforestation project

of the Instituto Terra. Red pixels stand for near-infrared light and vegetation, while grey and green and darker pixels indicate an absence of vegetation.

Figure 3: Instituto Terra - Infrared Composite Images



Notes. This figure reports the infrared composite images for the site of the Instituto Terra before and after the site was built (3-km radius). The first image was obtained by compressing all images available in the window 1997-2000. The compression minimized the presence of clouds. The same procedure was applied to obtain the second image over the window 2009-2012 (end of the dataset). Red pixels stand for near-infrared light and vegetation, while gray and green pixels indicate an absence of vegetation.

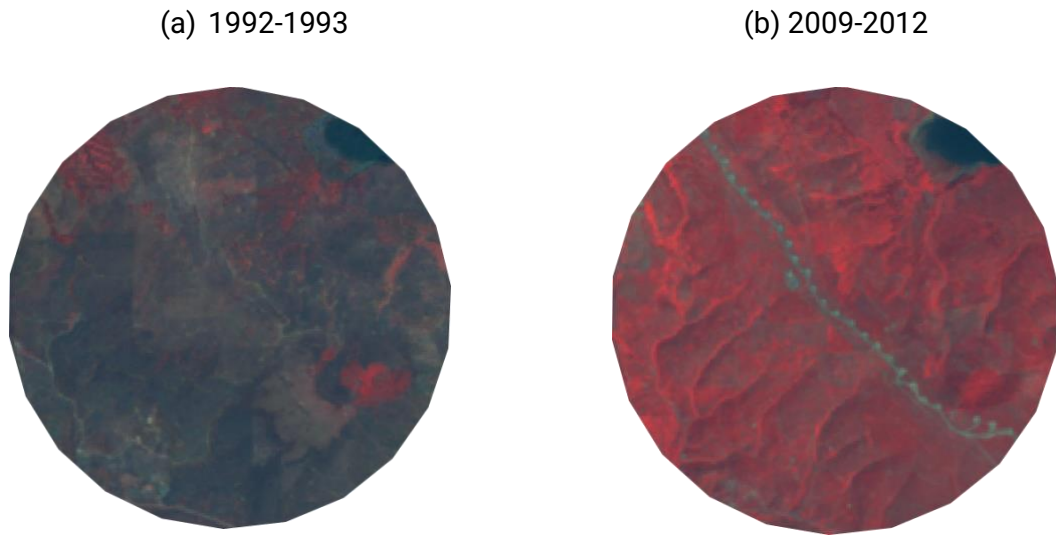
If we move from before (Panel a) to after (Panel b) the reforestation project, we see that darker pixels (absence of vegetation) leave space to red pixels (presence of vegetation). We use these images to build the EVI values reported in the paper.

4 IMAGES AND FIGURES FOR FOUNTAIN WILDFIRE

Nature-positive projects are more difficult to analyse, especially when reforestation is done in the aftermath of a wildfire. While the nature-negative companies and assets are more alike - i.e. an extraction site that damages vegetation -, nature-positive initiatives and their characteristics are more heterogeneous. As a result, the choice of the time window to collect the images before the reforestation and the control location might depend significantly on the specific characteristics of the reforestation in question. In the case of a wildfire, the first considered time window moves to just after the event (rather than just before), and the time spread of the window we consider for the analysis must be fairly short to avoid capturing the beginning of the reforesting process. In addition, as a control location we would need an area that was destroyed by the fire and that was not restored. As in many cases the reforestation project restored the entirety of the site, it is not possible to find such control. One approach can thus be to consider a location destroyed by another wildfire that was not restored, with the caveat that this other location might have very different characteristics.

The Fountain wildfire. To document this aspect, we consider the reforestation project in the aftermath of the Fountain wildfire, a large and destructive wildfire that happened in 1992 in California [19]. Figure 4 shows the infrared composite images for these two windows:

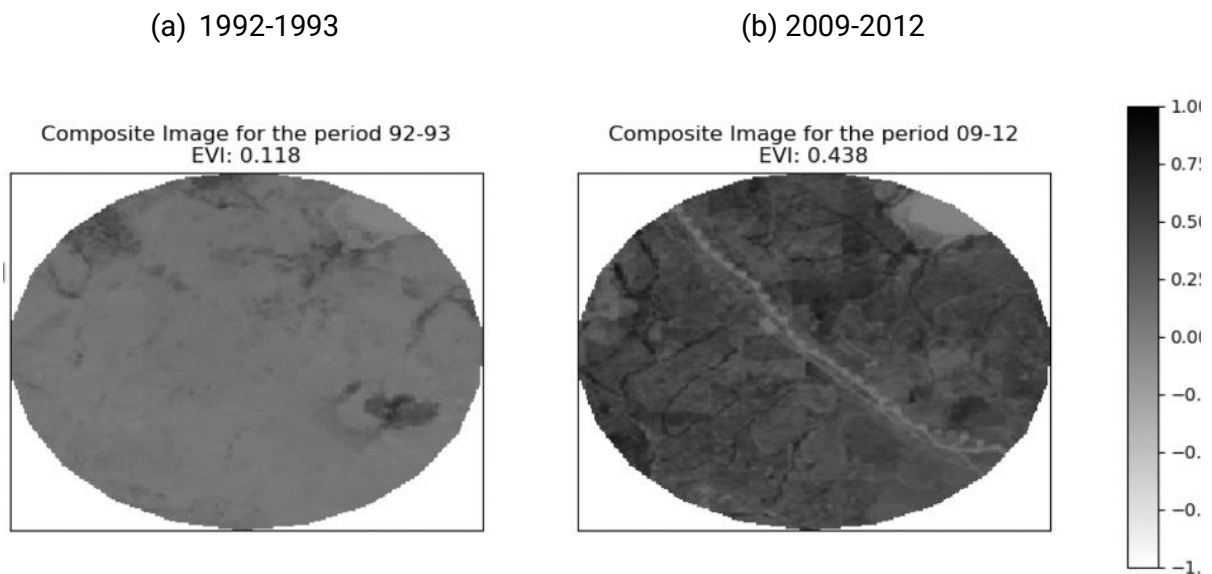
Figure 4: Fountain Wildfire - Infrared Composite Images



Notes. This figure reports the infrared composite images for the site of the Fountain wildfire just after the wildfire took place and after the reforestation (3-km radius). The first image was obtained by compressing all images available in the window 1992-1993. The compression minimized the presence of clouds. The same procedure was applied to obtain the second image over the window 2009-2012 (end of the dataset). Red pixels stand for near-infrared light and vegetation, while gray and green pixels indicate an absence of vegetation.

The difference is clear, as we move from an absence of vegetation in Panel (a) to a full reforestation in Panel (b). We then use these images to compute the EVI values, as it is reported in Figure 5:

Figure 5: Fountain Wildfire - Changes in the Enhanced Vegetation Index



Notes. This figure reports the values at the pixel level for the Enhanced Vegetation Index in images of the area of the site of the Fountain wildfire just after the fire took place (panel a) and after the reforestation (panel b) (3-km radius). Darker pixels are for positive EVI values (presence of vegetation), while clearer pixels are for negative EVI values (absence of vegetation).

The EVI reflects the reforestation process, as it moves from 0.118 just after the wildfire to 0.438 at the end of the reforestation process. This increase corresponds to a 271% increase, as it's reported in Column 1 of Table 2.

Table 2: Adjusted Difference in Enhanced Vegetation Index for Fountain Wildfire

	Fountain Location	Fountain Control Location
1992–93	0.1179	
2003–06		0.1254
2009–12	0.4383	0.1497
Diff	0.3204	0.0243
Diff %	271.7557	19.378
Diff-in-Diff	0.2961	

Notes. Columns 1 reports the baseline figures. Columns 2 and 3 report the figures obtained by changing the radius of the area of interest from 3 km to, respectively, 2 km and 4 km. Column 4 shows the results when we change the window used to compute the EVI value for before the mine was built from a time window just before the mine was built (1994-97) to a time window at the beginning of our dataset (1984-87). Columns 5 and 6 report the results as we change the time windows to obtain the EVI values from 3-year spans (1994-97 and 2009-12) to, respectively, 2-year spans (1995-1997 and 2010-2012) and 4-year spans (1993-97 and 2008-12).

Table 2 also shows the comparison with a control location. In the case of wildfires, the control location would need to be an area that was destroyed by the wildfire (as our area of interest), but that was not reforested. In the case of the Fountain wildfire, all the areas affected by the fire were reforested, and therefore we do not dispose of a control location “nearby” our area of interest – as we did for the cases of Antamina and Instituto Terra. One way to address this challenge is picking a non-adjacent area that was affected by another wildfire, and that was never restored. Here we run this exercise by picking as control one area affected by the Hayman site, Colorado, which was completely burned down in 2002 and never restored.¹³ Column 2 reports the evolution of the EVI for this location. In this case, we have used 3-year windows for both beginning (just after the wildfire happened) and end period, as no reforestation took place. In this control location the EVI presents a “slight” increase from 0.1254 to 0.1497 (19%), which is probably due to the natural reforestation taking place in the aftermath of wildfires. Applying the usual logic, we can then correct the change in the Fountain area with this naturally induced increase in vegetation in the Hayman site. The adjusted change for the Fountain site amounts to 0.2961 EVI points (rather than 0.3204).

This example shows one approach to address the absence of a control location in the context of wildfires. The important caveat here is that we are comparing potentially different plots of

¹³ The latitude and longitude coordinates are, respectively, 39.272829 and -105.252479.

lands, with very different characteristics and type of vegetation. This is why, in the ideal case, it would be better to have an area affected by the same wildfire that was not restored.

5 INSTITUTO TERRA: FINANCIAL REPORTS

In this section we report the information we gathered from the financial reports of the Instituto Terra. All reports are available at this link: <https://institutoterra.org/relatorio-financeiro/>. Table 3 summarizes all the figures, both in the original Reais currency (Panel a) and in US Dollars (Panel b).

Table 3: Instituto Terra – Financial Reports

Panel (a)

Thousand Reais	2001	2002	2003	2004	2005	2006	2007	2008	2009	2010	2011	2012
Operating (including reforestation)	-109	-187	-179	-1241								
Reforestation					-429	-897	-749	-296	-1141	-874	-885	-1398
Nursery					-106	-173	-469	-459	-762	-985	-826	-542
Education					-273	-702	-559	-199	-330	-1476	-658	-192
Fundraising / Projects					-248	-211	-308	-256	-226	-161	-172	-109
Environmental Extension											-228	-863
Administrative				-405	-624	-619	-462	-478	-351	-404	-372	-362
Salaries	-182	-374	-477									
Social Charges	-63	-141	-180									
Third-Party Services	-41	-117	-199									
General Expenses	-70	-190	-209									
Depreciation		-66	-115	-143	-175	-174	-182	-189	-191	-211	-230	-219
Financial, net	29	24	67	44	86	26	-13	-1	-16	-2	16	1
Other Expenses												-65
Total	-436	-1051	-1292	-1745	-1769	-2750	-2742	-1878	-3017	-4113	-3355	-3749
Total Cumulative	-436	-1487	-2779	-4524	-6293	-9043	-11785	-13663	-16680	-20793	-24148	-27897

Panel (b)

Thousand Dollars	2001	2002	2003	2004	2005	2006	2007	2008	2009	2010	2011	2012
Exchange rate (10.02.2023)	0.19											
Operating (including reforestation)	-20.71	-35.53	-34.01	-235.79								
Reforestation					-81.51	-170.43	-142.31	-56.24	-216.79	-166.06	-168.15	-265.62
Nursery					-20.14	-32.87	-89.11	-87.21	-144.78	-187.15	-156.94	-102.98
Education					-51.87	-133.38	-106.21	-37.81	-62.7	-280.44	-125.02	-36.48
Fundraising / Projects					-47.12	-40.09	-58.52	-48.64	-42.94	-30.59	-32.68	-20.71
Environmental Extension											-43.32	-163.97
Administrative				-76.95	-118.56	-117.61	-87.78	-90.82	-66.69	-76.76	-70.68	-68.78
Salaries	-34.58	-71.06	-90.63									
Social Charges	-11.97	-26.79	-34.2									
Third-Party Services	-7.79	-22.23	-37.81									
General Expenses	-13.3	-36.1	-39.71									
Depreciation		-12.54	-21.85	-27.17	-33.25	-33.06	-34.58	-35.91	-36.29	-40.09	-43.7	-41.61
Financial, net	5.51	4.56	12.73	8.36	16.34	4.94	-2.47	-0.19	-3.04	-0.38	3.04	0.19
Other Expenses												-12.35
Total	-82.84	-199.69	-245.48	-331.55	-336.11	-522.5	-520.98	-356.82	-573.23	-781.47	-637.45	-712.31
Total Cumulative	-82.84	-282.53	-528.01	-859.56	-1195.67	-1718.17	-2239.15	-2595.97	-3169.2	-3950.67	-4588.12	-5300.43

Notes. This table reports information from the financial statements of the Instituto Terra during the time we consider for our analysis, i.e. 2001-2012. Panel (a) reports the original figures in Brazilian Reais. Panel (b) reports the figures in US Dollars, converted with an exchange rate of 0.19 (from 10.02.2023). More information can be found here: <https://institutoterra.org/relatorio-financeiro/>.

Our goal here is to track the amount of money that was used to finance the restoration project of the Instituto Terra, during the period of analysis. As we observe changes from the start of the operations in 2001 to the end of our dataset in 2012, we consider financial figures over 2001-2012. The Instituto Terra works as a foundation, i.e. it receives funds from donors and it

uses them to finance the reforestation of the rain forest in the area of operations. Aside from this core activity, the Instituto Terra runs a series of auxiliary activities, such as education.¹⁴

The financial reports of the Instituto Terra provide the split between operating expenses, administrative expenses, depreciation, financial and other expenses. The split for reforestation expenses is included within operating expenses from 2005 onwards and varies between US\$ 56,000 in 2008 to US\$ 265,000 in 2012. The overall amount of expenses is reported in the last line of Table 3, with a cumulated amount for the period of US\$5.3 million.

We use these figures as an estimate of how much it comprehensively costs to restore and preserve the amount of vegetation restored by the Instituto Terra, and therefore the amount of vegetation damaged by the Antamina mining site. We argue that the best approach is to consider the overall expenses of the Instituto, rather than only the expenses dedicated to reforestation. The main reason being that all the auxiliary expenses are fundamental for the centre's existence, which depends on the work of its employees and other activities such as education. We thus use the figure of US\$ 5.3 million as our baseline estimates for the comprehensive costs of reforestation, and therefore the proportioned cost for the vegetation loss produced by the Antamina mine, as explained in the white paper. As an alternative, we could consider different cuts of operating expenses of the Instituto.

This example shows how we could independently gather financial information from restoration projects and use it to estimate the cost of vegetation loss. In future work, we will gather a sample of projects, including their financial reports, and compute averages of operating expenses within this sample, with the goal to obtain estimates that do not depend on a single case.

6 REFERENCES

- [1] Q. Weng, 'A remote sensing?GIS evaluation of urban expansion and its impact on surface temperature in the Zhujiang Delta, China', *Int. J. Remote Sens.*, vol. 22, no. 10, pp. 1999–2014, Jan. 2001, doi: 10.1080/713860788.
- [2] M. C. Hansen et al., 'High-Resolution Global Maps of 21st-Century Forest Cover Change', *Science*, vol. 342, no. 6160, pp. 850–853, Nov. 2013, doi: 10.1126/science.1244693.
- [3] Google Earth Engine, 'A planetary-scale platform for Earth science data & analysis', *Google Earth Engine*, 2023. <https://earthengine.google.com/> (accessed Feb. 09, 2023).
- [4] L. Betz, 'Landsat 5 Sets Guinness World Record For "Longest Operating Earth Observation Satellite"', *NASA*, Feb. 10, 2013. https://www.nasa.gov/mission_pages/landsat/news/landsat5-guinness.html (accessed Feb. 09, 2023).
- [5] Google Earth Engine, 'Landsat 5', *Google Earth Engine - Landsat 5*, 2023. <https://developers.google.com/earth-engine/datasets/catalog/landsat-5> (accessed Feb. 09, 2023).
- [6] Google Earth Engine, 'Sentinel 2', *Google Earth Engine - Sentinel 2*, 2023. <https://developers.google.com/earth-engine/datasets/catalog/sentinel-2> (accessed Feb. 09, 2023).
- [7] J. W. Rouse, 'Monitoring the vernal advancement and retrogradation (green wave effect) of natural vegetation', *NASA*, 2013. [Online]. Available: <https://ntrs.nasa.gov/citations/19740022555>
- [8] N. Pettorelli, J. O. Vik, A. Mysterud, J.-M. Gaillard, C. J. Tucker, and N. Chr. Stenseth, 'Using the satellite-derived NDVI to assess ecological responses to environmental change', *Trends Ecol. Evol.*, vol. 20, no. 9, pp. 503–510, Sep. 2005, doi: 10.1016/j.tree.2005.05.011.
- [9] D. M. Gates, *Biophysical Ecology*. in Springer Advanced Texts in Life Sciences. New York, NY: Springer New York, 1980. doi: 10.1007/978-1-4612-6024-0.
- [10] S. Huang, L. Tang, J. P. Hupy, Y. Wang, and G. Shao, 'A commentary review on the use of normalized difference vegetation index (NDVI) in the era of popular remote sensing', *J. For. Res.*, vol. 32, no. 1, pp. 1–6, Feb. 2021, doi: 10.1007/s11676-020-01155-1.
- [11] R. B. Myneni and G. Asrar, 'Atmospheric effects and spectral vegetation indices', *Remote Sens. Environ.*, vol. 47, no. 3, pp. 390–402, Mar. 1994, doi: 10.1016/0034-4257(94)90106-6.
- [12] S. R. Karlson, H. B. Anderson, R. Van Der Wal, and B. B. Hansen, 'A new NDVI measure that overcomes data sparsity in cloud-covered regions predicts annual variation in ground-based estimates of high arctic plant productivity', *Environ. Res. Lett.*, vol. 13, no. 2, p. 025011, Feb. 2018, doi: 10.1088/1748-9326/aa9f75.
- [13] L. Montandon and E. Small, 'The impact of soil reflectance on the quantification of the green vegetation fraction from NDVI', *Remote Sens. Environ.*, vol. 112, no. 4, pp. 1835–1845, Apr. 2008, doi: 10.1016/j.rse.2007.09.007.
- [14] A. Huete, K. Didan, T. Miura, E. P. Rodriguez, X. Gao, and L. G. Ferreira, 'Overview of the radiometric and biophysical performance of the MODIS vegetation indices', *Remote Sens. Environ.*, vol. 83, no. 1–2, pp. 195–213, Nov. 2002, doi: 10.1016/S0034-4257(02)00096-2.
- [15] D. Tanre, B. N. Holben, and Y. J. Kaufman, 'Atmospheric correction against algorithm for NOAA-AVHRR products: theory and application', *IEEE Trans. Geosci. Remote Sens.*, vol. 30, no. 2, pp. 231–248, Mar. 1992, doi: 10.1109/36.134074.

¹⁴ For more information, you can find the annual reports here: <https://institutoterra.org/relatorio-anual/>.

- [16] B. N. Holben, 'Characteristics of maximum-value composite images from temporal AVHRR data', *Int. J. Remote Sens.*, vol. 7, no. 11, pp. 1417–1434, Nov. 1986, doi: 10.1080/01431168608948945.
- [17] NASA, 'MODIS Collection 6.1 (C61) VegetationIndex Product User Guide', 2019. [Online]. Available: https://lpdaac.usgs.gov/documents/621/MOD13_User_Guide_V61.pdf
- [18] E. Burchfield, J. Nay, and J. Gilligan, 'Application Of Machine Learning To The Prediction Of Vegetation Health', *Int. Arch. Photogramm. Remote Sens. Spat. Inf. Sci.*, vol. XLI-B2, 2016, [Online]. Available: https://digitalcommons.usu.edu/cgi/viewcontent.cgi?article=2514&context=envs_facpub
- [19] California Department of Water Resources, 'California's Most Significant Droughts: Comparing Historical and Recent Conditions', 2015. [Online]. Available: https://cawaterlibrary.net/wp-content/uploads/2017/05/CalSignificantDroughts_v10_int.pdf